https://doi.org/10.5194/acp-2019-752
Preprint. Discussion started: 4 September 2019

Atmospheric Chemistry and Physics Discussions

Heterogeneous Formation of Particulate Nitrate under Ammonium-rich Regime during the high $PM_{2.5}$ events in Nanjing, China

Yu-Chi Lin[1,2,3], Yan-Lin Zhang[1,2,3*], Mei-Yi Fan[1,2,3], Mengying Bao[1,2,3]

[1.] Yale-NUIST Center on Atmospheric Environment, International Joint Laboratory on Climate and Environment Change, Nanjing University of Information Science and Technology, Nanjing, 210044, China.

[2.] Key Laboratory Meteorological Disaster; Ministry of Education & Collaborative Innovation Center on Forecast and Evaluation of Meteorological Disaster, Nanjing University of Information Science and Technology, Nanjing, 210044, China.

[3]. Jiangsu Provincial Key Laboratory of Agricultural Meteorology, College of Applied Meteorology, Nanjing University of Information Science & Technology, Nanjing 210044, China.

Corresponded to Yan-Lin Zhang (dryanlinzhang@outlook.com; zhangyanlin@nuist.edu.cn)

ABSTRACT

Particulate nitrate (NO_3^-) not only influences regional climates but also contributes to the acidification of terrestrial and aquatic ecosystems. In 2016 and 2017, four intensive on-line measurements of water-soluble ions in $PM_{2.5}$ were conducted in Nanjing City to investigate the potential formation mechanisms of particulate nitrate. During the sampling periods, NO_3^- was the most predominant species, accounting for 35 % of the total water-soluble inorganic ions, followed by SO_4^{2-} (33 %) and NH_4^+ (24 %). Significant enhancements of nitrate aerosols in terms of both absolute concentrations and relative abundances suggested that NO_3^- was a major contributing

https://doi.org/10.5194/acp-2019-752
Preprint. Discussion started: 4 September 2019

Atmospheric Chemistry and Physics Discussions

species to high-$PM_{2.5}$ events (hourly $PM_{2.5}$ ≧ 150 μg m^{-3}). High NO_3^- concentrations mainly occurred under NH_4^+-rich conditions, implying that the formation of nitrate aerosols in Nanjing involved NH_3. During the high-$PM_{2.5}$ events, the nitrogen conversion ratios (Fn) were positively correlated with the aerosol liquid water content (ALWC, R = 0.75, $p < .05$). Meanwhile, increasing NO_3^- concentrations regularly coincided with increasing ALWC and decreasing Ox (Ox = O_3 +NO_2). These results suggested that the heterogeneous reaction was probably a major mechanism of nitrate formation. Moreover, the average production rate of NO_3^- by heterogeneous processes was estimated to be 12.6 % h^{-1}, which was much higher than that (2.5 % h^{-1}) of gas-phase reactions. This can also explain the abrupt increase of nitrate concentrations during the high $PM_{2.5}$ events. Finally, ammonium nitrate aerosol formation was HNO_3-limited, indicating that the control of NOx emissions will be able to efficiently reduce airborne nitrate concentrations and improve the air quality in this industrial city.

Keywords: Nitrate aerosols, nitrogen conversion ratios, NH_4^+-rich regime, Hydrolysis of N_2O_5, Nitrate production rate

1. Introduction

Due to the rapid growth of industrialization and urbanization, particulate matter (PM) pollution has become a series problem in China in recent years (Chan and Yao, 2008; Zhang and Cao, 2015). Fine mode particles ($PM_{2.5}$, with aerodynamic diameters less than 2.5 μm) exhibit smaller sizes and contain many toxins emitted from anthropogenic emissions. $PM_{2.5}$ easily penetrates the upper respiratory tract and is deposited into the human body, causing serious threats to human health. Numerous previous studies have proven that people exposed to high $PM_{2.5}$ concentrations show increased risks of respiratory illness, cardiovascular diseases and asthma (Brauer et

https://doi.org/10.5194/acp-2019-752
Preprint. Discussion started: 4 September 2019


Atmospheric Chemistry and Physics Discussions

al., 2002; Defino et al., 2005), resulting in an increase of mortality (Nel, 2005).

Secondary inorganic aerosols (SIA), including sulfate (SO_4^{2-}), nitrate (NO_3^-) and ammonium (NH_4^+), are major constituents of $PM_{2.5}$, accounting for 25 - 58 % of the $PM_{2.5}$ mass in urban cities of China (Huang et al.,2014a; Wang et al., 2018; Yang et al., 2005; Ye et al., 2017; Zhao et al., 2013; Zhou et al., 2018). Among these species, SO_4^{2-} and NO_3^- are acidic ions which tend to be neutralized by NH_4^+. Previously, many studies suggested that SO_4^{2-} dominated SIA in urban cities of China (Kong et al., 2014; Tao et al., 2016; Yang et al., 2005; Yao et al., 2002; Zhao et al., 2013). In recent years, the Chinese government reduced its anthropogenic emissions by 62 % and 17 % for SO_2 and NOx (Zheng et al., 2018). This revealed that the reduction efficiency of SO_2 emissions were much higher than those of NOx. Consequently, nitrate has become the dominant species of SIA, especially during PM haze events (Wang et al., 2018; Wen et al., 2015; Zou et al., 2018).

In the atmosphere, ammonium nitrate (NH_4NO_3) is a major form of nitrate aerosols in fine mode particles. NH_4NO_3 is a semi-volatile species which partitions from the particle phase into the gas phase under high-temperature (T) conditions. It deliquesces when the ambient relative humidity (RH) is higher than its deliquescence relative humidity (DRH, nearly 62 % RH at atmospheric standard condition). To produce NH_4NO_3, nitrogen oxides (NO_x) and ammonia (NH_3) undergo a series of chemical reactions. NO_x mostly emits as fresh NO, which is subsequently oxidized to NO_2 and reacts with hydrogen oxide (OH) radicals to generate nitric acid (HNO_3), and then HNO_3 reacts with NH_3 to yield NH_4NO_3 particles as listed in R1 and R2 (Calvert and Stockwell, 1983). Particulate NH_4NO_3 formation rate is profoundly dependent on the ambient T and RH since both parameters influence the equilibrium constant ($P_{HNO3} \cdot P_{NH3}$) of NO_3^- and NH_4^+ between the particle and gas phases, as listed in R2 (Lin and Cheng, 2007).

https://doi.org/10.5194/acp-2019-752
Preprint. Discussion started: 4 September 2019

Atmospheric Chemistry and Physics Discussions

$$NO_{2(g)} + OH_{(g)} \rightarrow HNO_{3(g)} \quad k1 \quad (R1)$$

$$HNO_{3(g)} + NH_{3(g)} \rightarrow NH_4NO_{3(s,\,aq)} \quad k2 \quad (R2)$$

$$k_2 = [HNO_{3(g)}]\,[NH_{3(g)}] \quad (1)$$

Here, k_1 and k_2 are the reaction rate and equilibrium constant of R1 and R2, respectively. The equilibrium constant k_2 can be expressed as the product of HNO_3 and NH_3.

Heterogeneous reactions have been considered an important mechanism of nitrate formation during the nighttime. As listed in R3, liquid HNO_3 is produced by the hydrolysis of dinitrogen pentoxide (N_2O_5) on aerosol surfaces (Brown & Stutz, 2012; Chang et al., 2011; Mental et al., 1999; Wahner et al., 1998). Liquid HNO_3 can be neutralized by NH_4^+, which is produced from the conversion of gaseous NH_3. Nitrate aerosols yielded from both R2 and R3 require NH_3, and we can therefore consider these processes of NO_3^- formation to occur under NH_4 -rich conditions. Sometimes, there is not enough NH_3 to react with HNO_3 after complete neutralization by H_2SO_4. Under this condition, HNO_3 tends to react with other alkaline species such as Ca-rich dust ($CaCO_3$), and subsequently, nitrate aerosol is produced under a NH_4^+-poor regime (Goodman et al., 2000).

$$N_2O_{5(g)} + H_2O_{(l)} \rightarrow 2HNO_{3(aq)} \quad (R3)$$

The Yangtze River Delta (YRD) region is one of the well-known polluted areas in China (Zhang and Cao, 2015). Different from the case of dramatic elevated sulfate aerosol levels in Beijing (Wang et al., 2016), nitrate aerosols seemed to be a major contributing species during haze days in the YRD region (Wang et al., 2015; Wang et al., 2018). The formation mechanisms of nitrate in Nanjing have not yet been well understood, especially during high PM events. In this study, four intensive online measurements of water-soluble ions in $PM_{2.5}$ were conducted in Nanjing City in 2016

https://doi.org/10.5194/acp-2019-752
Preprint. Discussion started: 4 September 2019

Atmospheric Chemistry and Physics Discussions

and 2017. The data provided information on the hourly evolution of water-soluble inorganic ions (WSIIs) in the industrial city. The NO_3^- distributions under different NH_4^+ regimes (NH_4^+-poor and NH_4^+-rich conditions) were also discussed. Finally, we investigated the potential formation mechanisms of nitrate aerosols and their production rates during high-$PM_{2.5}$ events based on the online measurements.

2. Methodology

2.1 Sampling site

Particulate WSIIs and gaseous pollutants were continuously monitored at Nanjing University of Information Science and Technology (NUIST) located in the northern part of Nanjing City (see Figure 1). In addition to the contributions from vehicle emissions, petroleum chemical refineries and steel manufacturing plants are situated in the northeast and east direction at a distance of approximately 5 km. Four intensive campaigns were conducted from March 2016 to August 2017. During each experiment, the hourly concentrations of WSIIs in $PM_{2.5}$ and gaseous pollutants were continuously observed. Meanwhile, the hourly $PM_{2.5}$, NO_2 and O_3 concentrations along with the ambient T and RH were acquired from the Pukou air quality monitoring station which is located to the southwest of the receptor site.

2.2 Instruments

To monitor the hourly concentrations of WSIIs (Cl^-, NO_3^-, SO_4^{2-}, Na^+, NH_4^+, K^+, Mg^{2+} and Ca^{2+}), an online Monitor for Aerosols and Gases (MAGAR, Applikon-ENC, The Netherlands) instrument with a $PM_{2.5}$ inlet was employed. Using this instrument, the WSIIs in $PM_{2.5}$ were collected by a stream jet aerosol collector, while acidic (HCl, HONO, HNO_3 and SO_2) and basic gases (NH_3) were dissolved in a hydrogen peroxide solution on a wet rotation denuder (ten Brink et al., 2007; Griffith, et al., 2015). The

https://doi.org/10.5194/acp-2019-752
Preprint. Discussion started: 4 September 2019

Atmospheric Chemistry and Physics Discussions

liquid samples were then collected with syringe pumps and analyzed by ion chromatography (IC). Before each campaign, a seven-point calibration curve of each species was made, and an internal standard solution (LiBr) was used to check instrumental drifts. The method detection limits (MDLs) of Cl^-, NO_3^-, SO_4^{2-}, Na^+, NH_4^+, K^+, Mg^{2+} and Ca^{2+} were, 0.01, 0.04, 0.06, 0.05, 0.05, 0.07, 0.05 and 0.11 μg m^{-3}, respectively. For gases, the MDLs were 0.07, 0.09, 0.06, 0.02 and 0.08 μg/m^3 for HCl, HONO, HNO_3, SO_2 and NH_3, respectively.

2.3 ISORROPIA-II model

In this work**,** we used the ISORROPIA-II model to calculate the aerosol liquid water content (ALWC). ISORROPIA II is a thermodynamic equilibrium model which was built based on the Na^+ - Cl^- - Ca^{2+} - K^+ - Mg^{2+} - SO_4^{2-} - NH_4^+ - NO_3^- - H_2O aerosol system (Fountoukis & Nenes, 2007). This model has been successfully used to estimate the liquid water content in aerosols (Bian et al., 2014; Guo et al., 2015; Liu et al., 2017). The input parameters of ISORROPIA-II included the concentrations of WSIIs and their gaseous precursors (HNO_3, HCl and NH_3) as monitored by a MARGA instrument, together with the ambient T and RH. Here, the model was computed as a "forward problem", in which the quantities of aerosol- and gas-phase compositions along with the T and RH were well known. Additionally, the modeled values were determined using the "metastable" mode, which indicated that the aerosol compositions were assumed to be composed of an aqueous solution (Liu et al., 2017). The details of this model can be found elsewhere (Fountoukis and Nenes, 2007).

3. Results and discussion

3.1 Overview of water-soluble inorganic ions

Four intensive online measurements of WSIIs in $PM_{2.5}$ were carried out in

https://doi.org/10.5194/acp-2019-752
Preprint. Discussion started: 4 September 2019

Atmospheric Chemistry and Physics Discussions

Nanjing City from March 2016 to August 2017. Figure 2a plots the time series of the hourly $PM_{2.5}$ mass concentrations during the sampling periods. As seen, the hourly $PM_{2.5}$ mass concentrations varied from 5 to 252 μg m^{-3} with a mean value of 58 ± 35 μg m^{-3}. Compared with the 24-hour guideline (25 μg m^{-3}) suggested by the World Health Organization (WHO), our average $PM_{2.5}$ concentration (58 μg m^{-3}) was 2.3 times higher. This indicated that PM pollution in Nanjing City was a serious problem. During the campaigns, several high-$PM_{2.5}$ events with hourly $PM_{2.5}$ concentrations of higher than 150 μg m^{-3} were observed in the springtime and wintertime. These high $PM_{2.5}$ levels lasted for more than 3 hours, with obviously elevated NO_3^-. The details of nitrate formation during the high-$PM_{2.5}$ hours will be discussed in the following sections.

Figure 2b shows the time series of the hourly concentrations of SIA species, including SO_4^{2-}, NO_3^- and NH_4^+. The lack of data from March 7 to 14, 2016 was due to a malfunction of the MARGA instrument. During the sampling periods, the NO_3^- concentrations varied from 0.1 to 85.1 μg m^{-3} with a mean value of 16.7 ± 12.8 μg m^{-3}. The SO_4^{2-} concentrations ranged from 1.7 to 96.2 μg m^{-3} and averaged 14.9 ± 9.1 μg m^{-3}. The NH_4^+ concentrations fluctuated between 0.8 and 44.9 μg m^{-3} with a mean value of 10.7 ± 6.7 μg m^{-3}. On average, SIA counted for 91 % of the total water-soluble inorganic ions (TWSIIs) during the entirety of the sampling periods (see Figure 3a). Among these species, NO_3^- accounted for 35 % of the TWSIIs, followed by SO_4^{2-} (33 %) and NH_4^+ (24 %). The abundances of other ions, including Cl^-, K^+, Ca^{2+}, Na^+ and Mg^{2+}, were 5, 2, 1, 0.7 and 0.3 %, respectively. Figure S1 shows the scatter plot of the equivalent concentrations of the cations (Na^+, NH_4^+, K^+, Mg^{2+} and Ca^{2+}) and anions (Cl^-, SO_4^{2-} and NH_4^+). As seen, good correlations between cations and anions were found during the various sampling periods. The ratio of cation-to-anion was very close to 1.0 during each season, reflecting an ionic balance. This also

https://doi.org/10.5194/acp-2019-752
Preprint. Discussion started: 4 September 2019


Atmospheric Chemistry and Physics Discussions

indicated that our data exhibited good quality and was able to be used for the further analysis of scientific issues.

All SIA species exhibited similar seasonal patterns, with lower concentrations in the summer, especially for NO_3^-. The average concentrations of nitrate were 6.7 and 5.7 μg m^{-3} in the summertime of 2016 and 2017, respectively (see Figure S2). These values were much lower than those observed during other seasons. The local meteorological conditions, which were favorable for the dilution of air pollution, were one of the reasons for the declined NO_3^- concentrations during the hot seasons (Zhang and Cao, 2015). Another important reason for this effect was attributed to the formation process of $PM_{2.5}$ nitrate, which is very sensitive to the ambient temperature and relative humidity (Lin and Cheng, 2007). Figure S3a depicts the theoretical equilibrium constant ($P_{HNO3} \cdot P_{NH3}$) of partitioned NO_3^- and NH_4^+ between the particle and gas phase. Note that the *Y-axis* is presented on a log scale. The theoretical $P_{HNO3} \cdot P_{NH3}$ values increased exponentially with increasing ambient temperature but decreased with increasing RH. This indicated that NH_4NO_3 would be partitioned into the gas phase due to high equilibrium constants under high-temperature and low-RH conditions. Figure S3b illustrates the time series of the theoretical and observed $P_{HNO3} \cdot P_{NH3}$ values during the sampling periods. Obviously, higher theoretical equilibrium constants and lower observed $P_{HNO3} \cdot P_{NH3}$ values were found during the summer. This suggested that more NO_3^- and NH_4^+ would tend to be partitioned into the gas phase, resulting in lower particulate nitrate concentrations during hot seasons (Lin and Cheng, 2007).

Apart from seasonal variations, pronounced diurnal patterns were also found for SIA species (see Figure 4). NO_3^- exhibited similar diel cycles during different seasons, with higher concentrations in the early morning (4 a.m. - 8 a.m.) and lower levels between 2 p.m. and 5 p.m. The higher nitrate in the early morning might be due to

https://doi.org/10.5194/acp-2019-752
Preprint. Discussion started: 4 September 2019


Atmospheric Chemistry and Physics Discussions

enhanced nitrate formation in the residual layer in the mixing troposphere (Baasandorj et al., 2017; Prabhakar et al., 2017). The lower concentrations of nitrate during the daytime might be attributed to high temperatures, which inhibited the build-up of nitrate, especially during the summertime. In terms of sulfate, higher concentrations were observed between 6 am. and 1 p.m., indicating that the formation rate of sulfate was higher than the removal/dilution rate, leading to an increase of the sulfate concentration during the daytime. Nevertheless, the diurnal patterns of NH_4^+ mimicked those of NO_3^-, showing lower concentrations during the daytime. This was explained by the drastic decrease of particulate NH_4NO_3 concentrations under high temperatures and low relative humidity, resulting in lower NH_4^+ levels during the daytime.

3.2 Enhancements of nitrate at high $PM_{2.5}$ levels

Figure S4 shows the scatter plots of NO_3^-, SO_4^{2-} and NH_4^+ against $PM_{2.5}$. As seen, the slopes of NO_3^- (NO_3^- vs. $PM_{2.5}$ mass), SO_4^{2-} and NH_4^+ were 0.30, 0.24 and 0.19, respectively. This suggested that the increasing rate of NO_3^- during the high-$PM_{2.5}$ events was higher than those of other SIA species. At high $PM_{2.5}$ levels ($PM_{2.5} \geq$ 150 μg/m^3), NO_3^-, SO_4^{2-} and NH_4^+ contributed 39, 28 and 24 % of the TWSIIs, respectively (Figure 3b). However, the relative abundances of NO_3^-, SO_4^{2-} and NH_4^+ during low $PM_{2.5}$ concentrations (hourly $PM_{2.5} <$ 35 μg/m^3, see Figure 3c) were 29, 37 and 23 %, respectively. In recent years, dramatically enhanced amounts of nitrate aerosols during high-PM events have been observed at many urban sites in China (Wen et al., 2015; Wang et al., 2017; 2018; Zou et al., 2018). For instance, Zou et al. (2018) found that the nitrate concentrations during the occurrence of polluted air in Beijing and Tianjin were almost 14 times higher than those on relatively clean days ($PM_{2.5} <$ 75 μg/m^3), and the enhancement ratio of nitrate was much higher than that

https://doi.org/10.5194/acp-2019-752
Preprint. Discussion started: 4 September 2019

Atmospheric Chemistry and Physics Discussions

(5.3) of sulfate. Wang et al. (2018) noted that the enhancement ratio of NO_3^- (~6) between haze and clear days in Ningbo of the YRD region was much higher than that of SO_4^{2-} (~3). These findings suggested that NO_3^- was a major contributing species to fine particles during haze days since its increasing ratio between haze and non-haze days was much higher than those of other SIA species, such as sulfate and ammonium.

3.3 Nitrate formation under different ammonium regimes

Ammonium is a major species that neutralizes particulate SO_4^{2-} and NO_3^-. In the atmosphere, SO_4^{2-} competes with NO_3^- for NH_4^+ during their formation processes, and therefore, the relationship between the molar ratios of NO_3^-/SO_4^{2-} and NH_4^+/SO_4^{2-} can give us a hint for understanding the formation of NO_3^- under different ammonium regimes (Pathak et al., 2009; He et al., 2012; Tao et al., 2016). In an ammonium-rich regime, the HNO_3 produced by both gas oxidation and heterogeneous process reacts (or is neutralized) with "excess ammonium" at a NH_4^+/SO_4^{2-} molar ratio > 2 (theoretical value in an NH_4^+-rich regime) when sulfate is completely neutralized by NH_4^+ (Squizzato et al., 2013; Ye et al., 2011). In contrast, nitrate can be found under ammonium-poor conditions with a theoretical NH_4^+/SO_4^{2-} value that should be less than 2 (Pathak et al., 2009). Under NH_4^+-poor conditions, HNO_3 reacts with other cations, such as the calcium carbonate frequently found in natural dust.

Figure 5 shows the scatter plot of the molar ratios of NO_3^-/SO_4^{2-} against NH_4^+/SO_4^{2-}. It is found that good correlations exist between NO_3^-/SO_4^{2-} and NH_4^+/SO_4^{2-} under NH_4^+-rich regimes, with a correlation coefficient of 0.84 - 0.91. Utilizing the linear regression model, we suggested that nitrate aerosols (in NH_4^+-rich regimes) began to form when the NH_4^+/SO_4^{2-} molar ratios exceeded the criterion values of 1.7-2.0 during the different seasons (see in Table 1). The criterion values

https://doi.org/10.5194/acp-2019-752
Preprint. Discussion started: 4 September 2019

Atmospheric Chemistry and Physics Discussions

below 2 suggested that part of the sulfate might have existed in other forms, such as ammonium bisulfate. On the other hand, under ammonium-rich conditions, nitrate concentrations should be positively proportional to "excess ammonium" concentrations, a relationship which was defined as [excess-NH_4^+] = (NH_4^+/SO_4^{2-} - criterion value) × [SO_4^{2-}] (Pathak et al., 2009) (sulfate is in the units of nmol m^{-3} here). The criterion values were acquired from the regression models, as listed in Table 1. The results revealed that the excess NH_4^+ concentrations varied from -283 to 1422 nmol m^{-3} (see Figure 6), and only 1 % of the excess-NH_4^+ data were lower than zero, reflecting that NO_3^- formation in Nanjing occurred primarily under the NH_4^+-rich conditions. Moreover, the excess-NH_4^+ had apparent diurnal cycles, with higher concentrations in the early morning and lower concentrations at midday and in the early afternoon (see Figure 4, where we converted the units from nmol m^{-3} to μg m^{-3}). The diurnal patterns of NO_3^- mimicked those of the excess NH_4^+. This also suggested that particulate NO_3^- formation occurred mainly under NH_4^+-rich conditions. Figure 6 illustrates the relationship between the nitrate and excess NH_4^+ molar concentrations during the sampling periods. The nitrate molar concentrations correlated linearly with the excess NH_4^+ molar concentrations with a slope of approximately 1.0, which was consistent with the molar ratio of reaction between HNO_3 and NH_3. Interestingly, some scattered points were found in high ammonium concentrations (excess-NH_4^+ ≧ 900 nmol/m^3 ~ 16.2 μg/m^3), implying that residual NH_4^+ might be presented in another form such as NH_4Cl under high-NH_4^+ conditions. On the contrary, NO_3^- aerosols can be produced without involving NH_3; therefore, NO_3^- did not correlate well with the excess NH_4^+ under a NH_4^+-poor regime.

In this study, high nitrate concentrations were always found under NH_4^+-rich regimes, elucidating that nitrate during high PM levels in Nanjing were dominantly produced by the reaction of nitric acid (produced from NO_2 + OH and N_2O_5 + H_2O)

https://doi.org/10.5194/acp-2019-752
Preprint. Discussion started: 4 September 2019

Atmospheric Chemistry and Physics Discussions

with NH_3. Figure 6 also shows the nitrate concentrations against the excess NH_4^+ observed in various cities of China during the summertime (Pathak et al., 2009; Griffith et al., 2015). In Beijing and Shanghai, high nitrate concentrations during the summertime were found under NH_4^+-deficient conditions, which was very different from the findings of this work. In these studies (Pathak et al., 2009; Griffith et al., 2015), the high nitrate concentrations associated with NH_4^+-poor conditions might be due to the lower excess NH_4^+ concentrations under high-SO_4^{2-} conditions at that time since the strict control of SO_2 emissions started in 2013. In recent years, the reduction of anthropogenic SO_2 emissions decreased the airborne SO_4^{2-} concentrations, resulting in more excess NH_4^+ and leading to nitrate aerosol formation under NH_4^+-rich regimes. This argument can be supported by the recent results shown in Figure S5, in which high nitrate concentrations in Beijing were always found under NH_4^+-rich regimes.

3.4 Nitrate formation mechanism during high-$PM_{2.5}$ episodes

In this section, we attempted to explore the formation mechanisms of nitrate aerosols during high $PM_{2.5}$ levels. Here, nitrogen conversion ratio (Fn) was used to evaluate the conversion capability of NO_2 to total nitrate (gaseous and particulate NO_3^-), and it can be defined as (Khoder, 2002; Lin et al., 2006):

$$F_n = \frac{GNO_3^- + PNO_3^-}{GNO_3^- + PNO_3 + NO_2} \quad (1)$$

where GNO_3^- and PNO_3^- represent the NO_2 concentrations in nitric acid and particulate nitrate, respectively, with the units of μg m^{-3}. The results showed that the Fn values during the sampling periods varied from 0.01 to 0.57 with a mean value of 0.14 ± 0.09 (see Figure 2e). This value was comparable to that (0.17) in Taichung, an urban city in Taiwan, but was much higher than that (0.059) in Dokki, Egypt (Khoder,

https://doi.org/10.5194/acp-2019-752
Preprint. Discussion started: 4 September 2019


Atmospheric Chemistry and Physics Discussions

312 2002; Lin et al., 2006). On the other hand, Fn displayed significant diurnal cycles,
313 with the highest value in the early morning (see Figure 4). This enhanced Fn
314 coincided with increasing ALWC, suggesting heterogeneous reaction since ALWC is
315 one of the key parameters which favors the transformation of N_2O_5 to liquid HNO_3 in
316 this process. On the contrary, a second peak of Fn was found in the early afternoon
317 when Ox (Ox = NO_2 + O_3, an index of the oxidation capacity) concentrations
318 increased. This suggested that the total nitrate formation was attributed to the gas-
319 phase reaction of NO_2 + OH during the daytime.
320 Both gas-phase oxidation and heterogeneous reactions are potential pathways of
321 NH_4NO_3 formation. Here, we attempted to analyze the correlations of Fn vs. OH and
322 Fn vs. ALWC to investigate whether gas-phase oxidation or heterogeneous reactions
323 were the dominant mechanism of nitrate production. In this work, the OH radical
324 concentrations were not measured; hence, we used O_X as a proxy of OH. The ALWC
325 was obtained by computing the ISOPROPIA II model as described in section 2.3.
326 Figure 7 illustrates the scatter plots of Fn against Ox and ALWC during the high-
327 $PM_{2.5}$ events. As seen, Fn correlated well with the ALWC, with a correlation
328 coefficient (R) of 0.75 at a 95 % confidence level ($p < 0.05$). However, a poor
329 correlation was found between Fn and Ox. This elucidated that nitrate formation
330 during the high-$PM_{2.5}$ events in Nanjing was attributed to heterogeneous reactions
331 rather than to gas-phase processes. This result was consistent with recent conclusions
332 reached by oxygen isotope techniques, in which the hydrolysis of N_2O_5 in preexisting
333 aerosols was found to be a major mechanism of NO_3^- formation (Chang et al., 2018).
334
335 **3.5 Case study and formation rate of NO_3^- during $PM_{2.5}$ episodes**
336 Figure 8 shows several high-$PM_{2.5}$ events observed from March 3 to 6 in 2016.
337 In case I, the high $PM_{2.5}$ concentrations started at 6 p.m. on March 3 and ended at 3

https://doi.org/10.5194/acp-2019-752
Preprint. Discussion started: 4 September 2019


Atmospheric Chemistry and Physics Discussions

a.m. on March 4. During this event, the SO_4^{2-} and NH_4^+ concentrations remained at almost constant levels, but the NO_3^- concentrations revealed a slight enhancement. In the early morning of March 4, the NO_3^- concentrations increased from 39.4 to 47.8 μg m^{-3} within 4 hours, resulting in a nitrate production rate of 2.1 μg m^{-3} h^{-1} (~5.5 % h^{-1}, the calculation can be seen in the supplementary material). In case II, high $PM_{2.5}$ concentrations were observed from 8. a.m. to 2. p.m. on March 4. The NO_3^- concentrations were much higher than those of SO_4^{2-}, indicating nitrate-dominated aerosols. In this case, the NO_3^- concentrations increased from 38.1 to 51.2 μg m^{-3} within 6 hours, suggesting that the increasing rate of NO_3^- was 2.2 μg m^{-3} h^{-1} (2.4 % h^{-1}). Since the high NO_3^- concentrations occurred under high-Ox and low-ALWC conditions, this suggested that the gas-phase reaction of NO_2 + OH might be the dominant source of NO_3^- production in this event. In case III, a rapid growth of the $PM_{2.5}$ mass was found around midnight, along with a dramatic increase of NO_3^- concentrations from 11 p.m. on March 4 (31.0 μg m^{-3}) and maximizing at 1 a.m. the next day (64.5 μg m^{-3}). The increasing rate of NO_3^- was estimated to be 8.4 μg m^{-3} h^{-1} (~19.5 % h^{-1}), which was 4 times higher than those in case I and II. The high-nitrate event was found under increasing ALWC and decreasing Ox concentration conditions, suggesting that nitrate production occurred through heterogeneous processes. In case IV, the enhancements of all SIA species coincided with increasing ALWC and declining Ox concentrations. Again, the enhancement of nitrate was attributed to heterogeneous reactions rather than to gas-phase processes. In these events, the NO_3^- production rate was estimated to be 13.4 μg m^{-3} h^{-1} (~ 15.4 % h^{-1}).

Through the sampling periods, a total of twelve high $PM_{2.5}$ events was found, and the NO_3^- concentrations increased significantly during all the episodes (see in Table S1). Seven episodes suggested that heterogeneous processes (N_2O_5 + H_2O) might be a major pathway for nitrate formation since elevated NO_3^- levels coincided with

https://doi.org/10.5194/acp-2019-752
Preprint. Discussion started: 4 September 2019

Atmospheric Chemistry and Physics Discussions

increasing AWLC and decreasing Ox (or Ox remaining at a constant level). A level of approximately 70 % heterogeneous reactions was observed during the nighttime. In these events, the average NO_3^- production rate was 12.6 ± 7.3 % h^{-1}. On the contrary, NO_3^- concentrations rose with increasing Ox and decreasing ALWC in two $PM_{2.5}$ episodes. This finding indicated gas-phase processes (NO_2 + OH), and these gas-phase reaction cases occurred mainly during the daytime. The average production rate of NO_3^- in these events was 2.5 ± 0.1 % h^{-1}. Moreover, we also found some cases in which the elevated NO_3^- might have been from both gas-phase and heterogeneous reactions, and the corresponding NO_3^- formation rate was approximately 7.5 ± 3.0 % h^{-1}. In conclusion, enhancements of NO_3^- usually occurred under increased ALWC and decreased Ox conditions, indicating that heterogeneous reactions provided the dominant pathway of nitrate formation during the $PM_{2.5}$ episodes in Nanjing. Moreover, the average production rate of NO_3^- (12.6 % h^{-1}) by heterogeneous processes was 5 times higher than that (2.5 % h^{-1}) of gas-phase reactions. This might explain the abrupt increase of nitrate concentrations during the high $PM_{2.5}$ events.

3.6 NH_3/HNO_3 limitation of nitrate aerosol formation

In Nanjing, high nitrate concentrations occurred mainly under NH_4^+-rich regimes, indicating the involvement of atmospheric NH_3. This also demonstrated that both HNO_3 and NH_3 were crucial precursors for particulate nitrate formation. Assuming that NH_4NO_3 was the dominant form in $PM_{2.5}$ nitrate and that HNO_3+NH_3 was the major pathway for nitrate formation, we could then calculate the NH_4NO_3 concentrations from the observed total nitrate and ammonium concentrations by the following equation (Lin and Cheng., 2007):

$$[NH_4NO_3] = \left(\frac{[TNH_3]+[THNO_3]-\sqrt{([TNH_3]+[THNO_3])^2-4([TNH_3][THNO_3]-k_2)}}{2}\right) \quad (2)$$

https://doi.org/10.5194/acp-2019-752
Preprint. Discussion started: 4 September 2019

Atmospheric Chemistry and Physics Discussions

$$[NH_4NO_3] \leq \min([TNH_3], [THNO_3]) \quad (3)$$

where $[NH_4NO_3]$ is the ammonium nitrate concentration with a unit of ppb. $[TNH_3]$ and $[THNO_3]$ are the observed total ammonium (NH_3+excess-NH_4^+) and total nitrate (HNO_3+NO_3^-) concentrations, respectively. Both $[TNH_3]$ and $[THNO_3]$ are presented in units of ppb. k_2 is the equilibrium constant of reaction R2 with a unit of ppb^2. By using Eq. 2, we can estimate the $[NH_4NO_3]$ concentration with a unit of ppb^2, which is subsequently converted to μg m^{-3} under the specific ambient temperature and relative humidity.

During the sampling periods, the concentrations of total ammonium varied from 9.3 to 96.6 ppb with a mean value of 23.6 ppb. The concentrations of total nitrate ranged from 1.8 to 32.9 ppb with a mean value of 6.5 ppb. The average ratio of $[THNO_3]/[TNH_3]$ was 0.25. Figure 9 shows the contour plot of the NH_4NO_3 concentrations relative to the various NH_3 and HNO_3 levels calculated by Eq. 2. The observed total nitrate and ammonium concentrations are also plotted. As seen, the ridge line splits the plot into two parts; one is the NH_3-limited area (left), and the other is the HNO_3-limited area (right). In the current work, most of the observed data fell into the HNO_3-limited regime. This implied that the reduction of NOx emissions might be an important way to decrease airborne nitrate concentrations and ameliorate the air quality in Nanjing.

4. Conclusion and remarks

Four intensive online measurements of water-soluble ions in $PM_{2.5}$ were carried out in Nanjing City in 2016 and 2017 to realize the evolutions of SIA and the potential formation mechanisms of particulate nitrate. During the sampling periods, the average concentrations of NO_3^-, SO_4^{2-} and NH_4^+ were 16.7, 14.9 and 10.7 μg m^{-3}, respectively.

https://doi.org/10.5194/acp-2019-752
Preprint. Discussion started: 4 September 2019


Atmospheric Chemistry and Physics Discussions

This indicated that NO_3^- dominated the SIA. Significant seasonal variations and diurnal cycles were found for all SIA species. The low NO_3^- concentrations observed during the summer daytime could be attributed to the declined observed $P_{HNO3} \cdot P_{NH3}$ values under high-temperature conditions. Obvious enhancements of NO_3^- were found in terms of both absolute concentrations and relative abundances during the $PM_{2.5}$ episodes, indicating that NO_3^- was a major contributing species to $PM_{2.5}$. Different from the results obtained in Beijing and Shanghai, high nitrate concentrations always occurred under NH_4^+-rich regimes. The nitrogen conversion ratio, Fn, correlated well with the ALWC but not with Ox during high-$PM_{2.5}$ episodes. These findings indicated that NO_3^- aerosols at the receptor site were mainly produced by heterogeneous reactions ($N_2O_5 + H_2O$) with the involvement of NH_3. The average production rate of NO_3^- from heterogeneous reactions was estimated to be 12.6 % h^{-1}, which was 5 time higher than that of gas-phase reactions. According to the observations and calculations, particulate nitrate formation in Nanjing was HNO_3-limited, suggesting that the control of NOx emissions will be able to decrease the nitrate concentration and improve the air quality in this industrial city.

During the last decade, the mass ratios of nitrate-to-sulfate in $PM_{2.5}$ in the YRD region have been found to range from 0.3 to 0.7 (Lai et al., 2007; Wang et al., 2003; 2006; Yang et al., 2005; Yao et al., 2002), reflecting that the SO_4^{2-} concentration was much higher than the NO_3^- concentration. In the current study, the average mass ratio of nitrate-to-sulfate was 1.1. Indeed, high nitrate-to-sulfate mass ratios of > 1 were also observed in other mega-cities of China recently (Ge et al., 2017; Wei et al., 2018; Ye et al., 2017; Zou et al., 2018). The elevated nitrate-to-sulfate ratio should be due to the dramatic reduction of SO_2 emissions. The enhanced ratio also suggests that we should pay more attention to and develop some strategies for the reduction of NOx emissions, leading to declined nitrate concentrations in the atmosphere and

https://doi.org/10.5194/acp-2019-752
Preprint. Discussion started: 4 September 2019

Atmospheric Chemistry and Physics Discussions

441 improvement of the air quality in China.

442

443 **Data availability**

444 All the data used in this paper are available from the corresponding author upon

445 request (dryanlinzhang@outlook.com or zhangyanlin@nuist.edu.cn).

446

447 **Author contributions**

448 YLZ conceived and designed the study. YCL analyzed the data and wrote the

449 manuscript with YLZ. FM and MB performed aerosol sampling and data analyses

450 with YCL.

451

452 **Competing interests**

453 The authors declare that they have no conflict of interest.

454

455 **Acknowledgements**

456 This study was financially supported by the National Key R&D Program of China

457 (Grant No. 2017YFC0212704), the Natural Scientific Foundation of China (Nos.

458 91643109 and 41603104), the Provincial Natural Science Foundation of Jiangsu

459 (Grant No. BK20180040) and Jiangsu Innovation & Entrepreneurship Team.

460

461 **References**

462 Baasandorj, M., Hoch, S. W., Bares, R., Lin, J. C., Brown, S. S., Millet, D. B., Martin,

463 R., Kelly, K., Zarzana, K. J., Whiteman, C. D., Bube, W. P., Tonnesen, G.,

464 Jaramillo, J. C. and Sohl, J.: Coupling between chemical and meteorological

465 processes under persistent coal-air poor conditions: evolution of wintertime $PM_{2.5}$

466 events and N_2O_5 observation in Utah's Salt Lake Valley. *Environ. Sci. Technol.*,

https://doi.org/10.5194/acp-2019-752
Preprint. Discussion started: 4 September 2019

51, 5941-5950, https://doi.org/10.1021/acs.est.6b06603, 2017.

Brauer, M., Hoek, G., Vliet, V. P., Meliefste, K., Fischer, P. H., Wijga, A., Koopman, L. P., Neijens, H. J., Gerritsen, J., Kerkhof, M., Heinrich, J., Bellander, T., and Brunekreef, B.: Air pollution from traffic and the development of respiratory infections and asthmatic and allergic symptoms in children. *Am. J. Respir. Crit. Care Med.*, **166**, 1092-1098, https://doi.org/10.1146/rccm.200108-007OC, 2002.

Brown, S. S., and Stutz, J.: Nighttime radical observation and chemistry. *Chem. Soc. Rev.*, **41**, 6405-6447, https://doi.org/10.1039/c2cs35181a, 2012.

Calvert, J. G., and Stockwell, W. R.: Acid generation in the troposphere by gas-phase chemistry. *Environ. Sci. Technol.*, **17**, 428-443, https://doi.org/10.1021/es00115a727, 1983.

Chan, C. K., and Yao, X.: Air pollution in mega cities in China. *Atmos. Enviro.,* **42**, 1-42, https://doi.org/10.1016/j.atmosenv.2007.09.003, 2008.

Chang, W. L., Bhave, P. V., Brown, S. S., Riemer, N., Stutz, J., and Dabdub, D.: Heterogeneous atmospheric chemistry, ambient measurements, and model calculations of N_2O_5: a review. *Aerosol Sc. Technol.*, **45**, 655 - 685, https://doi.org/10.1080/02786826.2010.551672, 2011.

Defino, R. J., Siotuas, C., and Malik, S.: Potential role of ultrafine particles in associations between airborne particle mass and cardiovascular health. *Environ. Health Perspect.*, **113**, 934-938, https://doi.org/10.1289/ehp.7938, 2005.

Fountoukis, C., and Nenes, A.: ISORROPIA II: a computationally efficient thermodynamic equilibrium model for K^+-Ca^{2+}-Mg^{2+}-NH_4^+-Na^+-SO_4^{2-}-NO_3^--Cl^--H_2O. *Atmos. Chem. Phys.*, **7**, 4639-4659, https://doi.org/10.5194/acp-7-4639-2007, 2007.

Ge, X., Li, L., Chen, Y., Chen, H., Wu, D., Wang, J., Xie, X., Ge, S., Ye, Z., Xu, J., and Chen, M.: Aerosol characteristics and sources in Yangzhou, China resolved

https://doi.org/10.5194/acp-2019-752
Preprint. Discussion started: 4 September 2019


Atmospheric Chemistry and Physics Discussions

493 by offline aerosol mass spectrometry and other techniques. *Environ. Pollut.*, **225**,
494 74-85, https://doi.org/10.1016/j.encpol.2017.03.044, 2017.
495 Goodman, A. L., Underwood, G. M., and Grassian, V. H.: A laboratory study of the
496 heterogeneous reaction of nitric acid on calcium carbonate particles. *J. Geophys.*
497 *Res. Atmos.,* **105**, 29053-29064, https://doi.org/10.1029/2000JD900396, 2000.
498 Griffith, S. M., Huang, X. H. H., Louie, P. K. K., and Yu, J. Z.: Characterizing the
499 thermodynamic and chemical composition factors controlling $PM_{2.5}$ nitrate:
500 Insights from two years of online measurements in Hong Kong. *Atmos. Environ.*,
501 **122**, 864-875, https://doi.org/10.1016/ j.atmosenv.2015.02.009, 2015.
502 Guo, H., Xu, L., Bougiatioti, A., Cerully, K. M. , Capps, S. L., Heti Jr., J. R., Carton,
503 A. G., Lee, S.-H., Bergin, M. H., Ng, N. L., Nenes, A., and Weber, R. J.: Fine
504 particle water and pH in the southeastern United States. *Atmos. Chem. Phys.*, **15**,
505 5221-5228. https://doi.org/10.5194/acp-15-5211-2015, 2015.
506 He, K., Zhao, Q., Ma, Y., Duan, F., Yang, F., Shi, Z., and Chen, G.: Spatial and
507 seasonal variability of $PM_{2.5}$ acidity at two Chinese megacities: insights into the
508 formation of secondary inorganic aerosols. *Atmos. Chem. Phys.*, **12**, 1377-1395.
509 https://doi.org/10.5194/acp-12-1377-2012, 2012.
510 Huang, R.-J., Zhang, Y., Bozzetti, C., Ho, K.-F., Cao, J.-J., Han, Y., Daellenbach, R.,
511 Slowik, J. G., Platt, S. M., Canonaco, F., Zotter, P., Wolf, R., Pieber, S. M., Bruns,
512 E. A., Crippa, M., Ciarelli, G., Piazzalunga, A., Schwikkowski, M., Abbaszade,
513 G., Schnelle-Kreis, J., Zimmerman, R., An, Z., Szidat, S., Baltensperger, U.,
514 Haddad, I. E., and Prévôt, A. H.: High secondary aerosol contribution to
515 particulate pollution during haze events in China. *Nature*, **514**, 218-222,
516 https://doi.org/10.1038/nature13774, 2014a.
517 Huang, Y., Shen, H., Chen, H., Wang, R., Zhang, Y., Su, S., Chen, Y., Lin, N., Zhong,
518 Q., Wang, X., Liu, J., Li, B., Liu, W., and Tao, S.: Quantification of global primary

https://doi.org/10.5194/acp-2019-752
Preprint. Discussion started: 4 September 2019

519 emissions of $PM_{2.5}$, PM_{10} and TSP from combustion and industrial process sources.
520 *Environ. Sci. Technol.,* **48**, 13834-13843, https://doi.org/10.1021/es503696k,
521 2014b.
522 Khoder, M. I.: Atmospheric conversion of sulfur dioxide to particulate sulfate and
523 nitrogen dioxide to particulate nitrate and gaseous nitric acid in an urban area.
524 *Chemosphere*, **49**, 675-684, https://doi.org/10.1016/S0045-6535(02)00391-0,
525 2002.
526 Kong, L., Yang, Y., Zhang, S., Zhao, X., Du, H., Fu, H., Zhang, S., Cheng, T., Yang,
527 X., Chen, J., Wu, D., Sheng, J., Hong, S., and Jiao, L.: Observation of linear
528 dependence between sulfate and nitrate in atmospheric particles. *J. Geophys. Res.*
529 *Atmos.,* **119**, 341-361, https://doi.org/10.1002/2013JD020222, 2014.
530 Lin, Y.-C., and Cheng, M.-T.: Evaluation of formation rates of NO_2 to gaseous and
531 particulate nitrate in the urban atmosphere. *Atmos. Environ.,* **41**, 1903-1910,
532 https://doi.org/10.1016/j.atmosenv.2006.10.065, 2007.
533 Lin, Y.-C., Cheng, M.-T., Ting, W.-Y., and Yeh, C.-R.: Characteristics of gaseous
534 HNO_2, HNO_3, NH_3 and particulate ammonium nitrate in an urban city of central
535 Taiwan. *Atmos. Environ.,* **40**(25), 4725-4733,
536 https://doi.org/10.1016/j.atmosenv.2006.04.037, 2006.
537 Liu, M., Song, Y., Zhou, T., Xu, Z., Yan, C., Zheng, M., Wu, Z., Hu, M., Wu, Y., and
538 Zhu, T.: Fine particle pH during severe haze episodes in northern China.
539 *Geophys. Res. Lett.,* **44**, 5213-5222, https://doi.org/10.1002/2017GL073210,
540 2017.
541 Mental, T. F., Sohn, M., and Wahner, A.: Nitrate effect in the heterogeneous
542 hydrolysis of dinitrogen pentoxide on aqueous aerosols. *Phys. Chem. Chem.*
543 *Phys.*, **1**, 5451-5457, https://doi.org/10.1039/a905338g, 1999.
544 Nel, A.: Air pollution-related illness: effects of particles. *Science*, **308**, 804-806,

https://doi.org/10.5194/acp-2019-752
Preprint. Discussion started: 4 September 2019

https://doi.org/10.1126/science.1108752, 2005.

Pan, Y., Tian, S., Zhao, Y., Zhang, L., Zhu, X., Gao, J., Huang, W., Zhou, Y., Song, Y., Zhang, Q., and Wang, Y.: Identifying ammonia hotspots in China using a national observation work. *Environ. Sci. and Technol.*, **52**, 3926-3934. https://doi.org/10.1021.acs/est.7b05235, 2018.

Pathak, R. K., Wu, W. S., and Wang, T.: Summertime $PM_{2.5}$ ionic species in four major cities of China: nitrate formation in an ammonia-deficient atmosphere. *Atmos. Chem. and Phys.*, **9**, 1711-1722, https://doi.org/10.5194/acp-9-1711-2009, 2009.

Prabhakar, G., Parworth, C. L., Zhang, X., Kim, H., Young, D. E., Beyersdorf, A. J., Ziemba, L. D., Nowak, J. B., Bertram, T. H., Faloona, I. C., Zhang, Q., and Cappa, C. D.: Observational assessment of the role of nocturnal residual-layer chemistry in determining daytime surface particulate nitrate concentrations. *Atmos. Chem. Phys.*, **17** (23), 14747-14770, https://doi.org/10.5194/acp-17-14747-2017, 2017.

Squizzato, S., Masiol, M., Brunelli, A., Pistollato, S., Tarabotti, Z., Rampazzo, G., and Pavoni, B.: Factors determining the formation of secondary inorganic aerosol: a case study in the Po Valley (Italy). *Atmos. Chem. and Phys.,* **13**, 1927-1339, https://doi.org/10.5194/acp-13-1927-2013, 2013.

Tao, Y., Ye, X., Ma, Z., Xie, Y., Wang, R., Chen, J., Yang, X., and Jiang, S.: Insights into different nitrate formation mechanisms from seasonal variations of secondary inorganic aerosols in Shanghai. *Atmos. Environ.,* **145**, 1-9, https://doi.org/10.1016/j.atmosenv.2016.09.012, 2016.

ten Brink, H., Otjes, R., Jongejan, P., and Slanina, S.: An instrument for semi-continuous monitoring of the size-distribution of nitrate, ammonium, sulfate and chloride in aerosols. *Atmos. Environ.,* **41**, 2768-2779,

https://doi.org/10.5194/acp-2019-752
Preprint. Discussion started: 4 September 2019

https://doi.org/10.1016/j.atmosenv.2006.11.041, 2007.

Wahner, A., Mental, T. F., Sohn, M., and Stier, J.: Heterogenous reaction of N_2O_5 on sodium nitrate aerosol. *J. Geophys. Res. Atmos.*, **103**, 31103-31112, https://doi.org/10.1029/1998JD100022, 1998.

Wang, G., Wang, H., Yu, Y., Gao, S., Feng, J., Gao, S., & Wang, L.: Chemical characterization of water-soluble components of PM_{10} and $PM_{2.5}$ atmospheric aerosols in five locations of Nanjing, China. *Atmos. Environ.*, **37**., 2893-2902. https://doi.org/10.1016/j.atmosenv.S1352-2310(03)00271-1, 2003.

Wang, G., Zhang, R., Geomez, M. E., Yang, L., Zamora, M. L., Hu, M., Lin, Y., Peng, J., Guo, S., Meng, J., Li, J., Cheng, C., Hu, T., Ren, Y., Wang, Y., Gao, J., An, Z., Zhou, W., Li, G., Wang, J., Tian, P., Marrero-Ortiz, W., Secrest, J., Du, Z., Zheng, J., Shang, D., Zheng, L., Shao, M., Wang, W., Huang, Y., Wang, Y., Zhu, Y., Li, Y., Hu, J., Pan, B., Cai, L., Cheng, Y., Ji, Y., Zhang, F., Rosenfeld, D., Liss, P. S., Duce, R. A., Kolb, C. E., and Molina, M. J.: Persistent sulfate formation from London fog to Chinese haze. *Proc. Natl. Acad. Sci.*, **113**, 13630-13635, https://doi.org/ 10.1073/pnas.1616540113, 2016.

Wang, H., Lu, K., Chen, X., Zhu, Q., Chen, Q., Guo, S., Jiang, M., Li, X., Shang, D., Tang, Z., Wu, Y., Wu, Z., Zou, Q., Zheng, Y., Zheng, L., Zhu, T., Hu, M., and Zhang, Y.: High N_2O_5 concentrations observed in urban Beijing: implications of a large nitrate formation. *Environ. Sci. Technol. Lett.*, **4**, 416-420, https://doi.org/10.1021/acsestlett.7b00341, 2017.

Wang, H., Zhu, B., Shen, L., Xu, H., An, J., Xue, G., and Cao, J.: Water soluble ions in atmospheric aerosols measured in five sites in the Yantze River Delta, China: size-fractionated seasonal variation and sources. *Atmos. Environ.*, **123**(B), 370-379, https://doi.org/10.1016/j.atmosenv.2015.05.070, 2015.

Wang, W., Yu, J., Cui. Y., He, J., Xue, P., Cao, W., Ying, H., Gao, W., YIng, Y., Gao,

https://doi.org/10.5194/acp-2019-752
Preprint. Discussion started: 4 September 2019

W., Yan, Y., Hu, B., Xin, J., Wang, L., Liu, Z., Sun, Y., Ji, D., and Wang, Y.: Characteristics of fine particulate matter and its sources in an industrialized coastal city, Ningbo, Yantze River Delta, China. *Atmos. Res.*, **203**, 105-117, https://doi.org/10.1016/j.atmosres.2017.11.033, 2018.

Wang, Y., Zhuang, G., Zhang, X., Xu, C., Tang, A., Chen, J., and An, Z.: The ion chemistry, seasonal cycle, and sources of $PM_{2.5}$ and TSP aerosol in Shanghai. *Atmos. Environ.,* **40**(16), 2935-2952, https://doi.org/10.1016/j.atmosenv.2005.12.051, 2006.

Wei, L., Yue, S., Zhao, W., Yang, W., Zhang, Y., Ren, L., Han, X., Guo, Q., Sun, Y., Wang, Z., and Fu, P.: Stable sulfur isotope ratios and chemical compositions of fine aerosols ($PM_{2.5}$) in Beijing, China. *Sci. Total Environ.*, **633**, 1156-1164, https://doi.org/10.1016/j.scitotenv.2018.03.153, 2018.

Wen, L., Chen, J., Yang, L., Wang, X., Xu, C., Sui, X., Yao, L., Zhu, Y., Zhang, J., Zhu, T., and Wang, W.: Enhanced formation of particulate nitrate at a rural site on the North China Plain in summer: the importance roles of ammonia and ozone. *Atmos. Environ.,* **101**, 294-302, doi:10.1016/j.atmosenv.2014.11.037, 2015.

Yang, H., Yu, J. Z., Ho, S. S. H., Xu, J., Wu, W.-S., Wan, C. H., Wang, X., Wang, X., and Wang, L.: The chemical composition of inorganic and carbonaceous materials in $PM_{2.5}$ in Nanjing, China. *Atmos. Environ. ,* **39**, 3735-3749, https://doi.org/10.1016/j.atmosenv.2005.03.010, 2005.

Yao, X., Chan, C. K., Fang, M., Cadle, S., Chan, T., Mulawa, P., He, K., and Ye, B.: The water-soluble ionic composition $PM_{2.5}$ in Shanghai and Beijing, China. *Atmos. Environ.,* **36**, 4223-4234, https://doi.org/10.1016/j.atmosenv.2005.12.051, 2002.

Ye, X. N., Ma, Z., Zhang, J. C., Du, H. H., Chen, J. M., Chen, H., Yang, X., Gao, W., and Geng, F. H.: Important role of ammonia on haze formation in Shanghai.

https://doi.org/10.5194/acp-2019-752
Preprint. Discussion started: 4 September 2019

Environ. Res. Lett., **6**, 024019, https://doi.org/10.1088/1748-9326/6/2024019, 2011.

Ye, Z., Liu, J., Gu, A., Feng, F., Liu, Y., Bi, C., Xu, J., Li, L., Chen, H., Chen, Y., Dai, L., Zhou, Q., and Ge, X.: Chemical characterization of fine particulate matter in Changzhou, China and source apportionment with offline aerosol mass spectrometry. *Atmos. Chem. .Phys.,* **17**, 2573-2592, https://doi.org/10.5194/acp-17-2573-2017, 2017.

Zhang, Y.-L., and Cao, F.: Fine particulate matters ($PM_{2.5}$) in China at a city level. *Sci. Rep.,* **5**, 14884, https://doi.org/10.1038/srep14884, 2015.

Zhao, P. S., Dong, F., He, D., Zhao, X. J., Zhang, X. L., Zhang, W. Z., Yao, Q., and Liu, H. Y.: Characteristics of concentrations and chemical compositions for PM2.5 in the region of Beijing, Tianjin, and Hebei, China. *Atmos. Chem. Phys.,* **13**, 4631-4644, https://doi.org/10.5194/acp-13-4631-2013, 2013.

Zheng, B., Tong, D., Li, M., Liu, F., Hong, C., Geng, G., Li, H., Li, X., Peng, L., Qi, J., Yan, L., Zhang, Y., Zhao, H., Zheng, Y., He, K., and Zhang, Q.: Trends in China's anthropogenic emissions since 2010 as the consequence of clean air actions. *Atmos. Chem. .Phys.,* **18**(19), 14095-14111, https://doi.org/10.5194/acp-18-14095-2018, 2018.

Zou, J., Liu, Z., Hu, B., Huang, X., Wen, T., Ji, D., Liu, J., Yang, Y., Yao, and Wang, Y.: Aerosol chemical compositions in the Northern China Plain and the impact on visibility in Beijing and Tianjin., *Atmos. Res.*, **201**, 235-246, https://doi.org/10.1016/j.atmosres.2017.09.014, 2018.

https://doi.org/10.5194/acp-2019-752
Preprint. Discussion started: 4 September 2019

Atmospheric Chemistry and Physics Discussions

Table Captions

Table 1 The regression models between NO_3^-/SO_4^{2-} (Y) and NH_4^+/SO_4^{2-} (X) along with the criterion values of NH_4^+/SO_4^{2-} in ammonium-rich regime during the sampling periods.

Figure Captions

Figure 1 Relative locations of the sampling site**.** In this figure, the sampling site (Nanjing) by the red dot. The contour denotes $PM_{2.5}$ emission data (kg km^{-1} $month^{-1}$ which is obtained from Huang et al. (2014b).

Figure 2 Time series of concentrations in (a) $PM_{2.5}$ mass, (b) SIA species, (c) ALWC and (d) Ox along with (e) Fn observed in Nanjing during the sampling periods.

Figure 3 Abundance of each species in TWSIIs during the (a) entire, (b) haze ($PM_{2.5} \geq$ 150 μg m^{-3}) and (c) clear ($PM_{2.5} < 35$ μg m^{-3}) events. The numbers in the parentheses are standard deviations.

Figure 4 Diurnal variations of the concentrations of NO_3^-, SO_4^{2-} and NH_4^+, excess-NH_4^+, Ox and ALWC, and nitrogen conversion ratio (Fn) as well as ambient relative humidity in Nanjing during the sampling periods. For SO_4^{2-}, NO_3^- and NH_4^+, the mean values (dots) and standard deviations (solid lines) are plotted.

Figure 5 Scatter plots of molar ratios of NO_3^-/SO_4^{2-} against NH_4^+/SO_4^{2-} in Nanjing during the different seasons.

Figure 6 Scatter plot of NO_3^- vs. excess-NH_4^+ molar concentrations in Nanjing during the different seasons. The results in Beijing, Shanghai, Guangzhou, Lanzhou and Hong Kong are also shown in this figure.

https://doi.org/10.5194/acp-2019-752
Preprint. Discussion started: 4 September 2019

Atmospheric Chemistry and Physics Discussions

Figure 7 Scatter plots of (a) Fn against Ox and (b) Fn against ALWC during the high hourly $PM_{2.5}$ concentration conditions (hourly $PM_{2.5}$ $\geqq$ 150 μg m^{-3}).

Figure 8 Time series of concentrations in (a) $PM_{2.5}$ mass, (b) SIA species (NO_3^-, SO_4^{2-} and NH_4^+), (c) ALWC, Ox and NO_2 and (d) RH and T in Nanjing City from March 3 to 6, 2016. The grey shadows denote $PM_{2.5}$ episodes. The red numbers represent NO_3^- formation rate during the $PM_{2.5}$ episodes.

Figure 9 The isopleth of concentration in NH_4NO_3 aerosols (μg m^{-3}) versus NH_3 and HNO_3 concentrations (units in ppb). The NH_4NO_3 concentrations were calculated using Eq. 2 in the text. The dots denote the observed data.

https://doi.org/10.5194/acp-2019-752
Preprint. Discussion started: 4 September 2019

Atmospheric Chemistry and Physics Discussions

Table 1 The regression models between NO_3^-/SO_4^{2-} (Y) and NH_4^+/SO_4^{2-} (X) along with the criterion values of NH_4^+/SO_4^{2-} in ammonium-rich regime during the sampling periods.

Sampling periods	Regression models	Criterion values of NH_4^+/SO_4^{2-}
2016 spring	$Y = 0.71\ X - 1.27;\ R^2 = 0.87$	1.8
2016 summer	$Y = 0.67\ X - 1.22;\ R^2 = 0.86$	1.8
2017 winter	$Y = 0.81\ X - 1.50;\ R^2 = 0.91$	1.9
2017 spring	$Y = 0.95\ X - 1.91;\ R^2 = 0.94$	2.0
2017 summer	$Y = 0.79\ X - 1.32;\ R^2 = 0.84$	1.7

https://doi.org/10.5194/acp-2019-752
Preprint. Discussion started: 4 September 2019

Atmospheric Chemistry and Physics Discussions

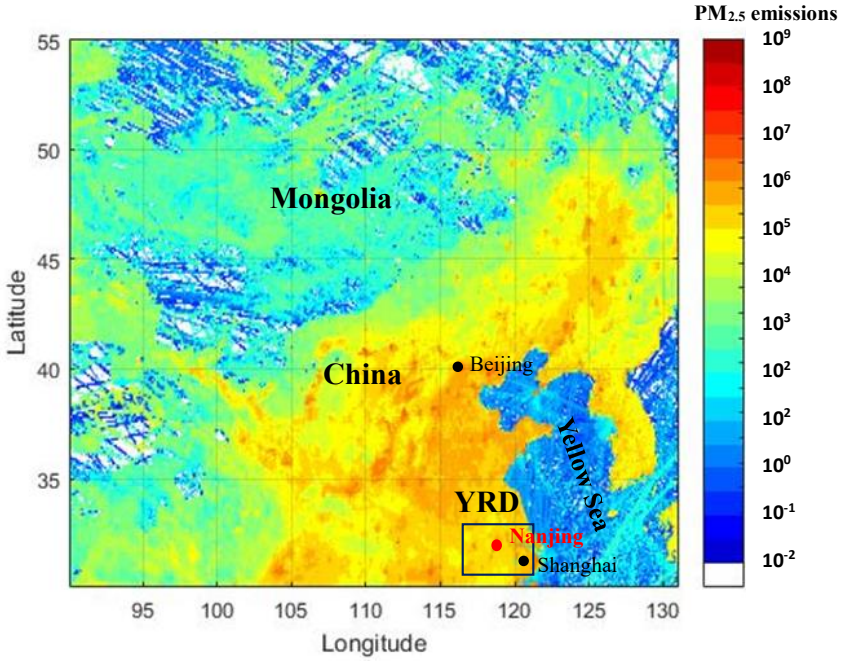

Figure 1 Relative locations of the sampling site**.** In this figure, the sampling site (Nanjing) by the red dot. The contour denotes $PM_{2.5}$ emission data (kg km^{-1} $month^{-1}$ which is obtained from Huang et al. (2014b).

https://doi.org/10.5194/acp-2019-752
Preprint. Discussion started: 4 September 2019

Atmospheric Chemistry and Physics Discussions

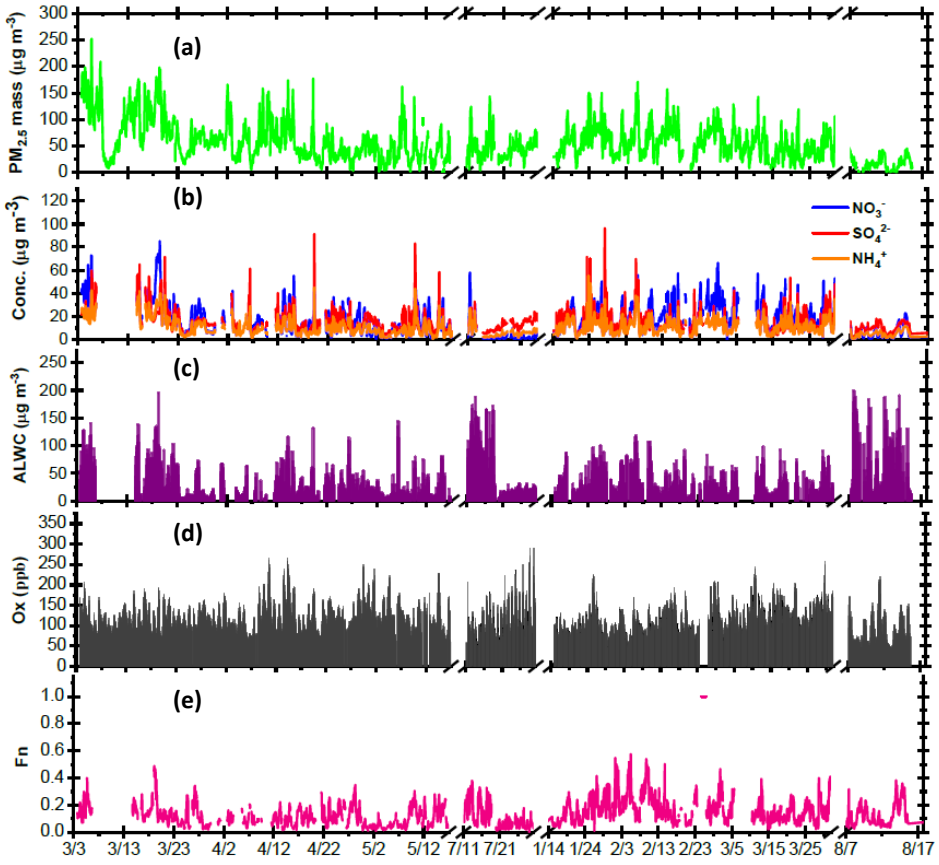

Figure 2 Time series of concentrations in (a) $PM_{2.5}$ mass, (b) SIA species, (c) ALWC and (d) Ox along with (e) Fn observed in Nanjing during the sampling periods.

https://doi.org/10.5194/acp-2019-752
Preprint. Discussion started: 4 September 2019

Atmospheric Chemistry and Physics Discussions

(a) Entire days: $PM_{2.5}$ = 58 ± 35 μg m^{-3}

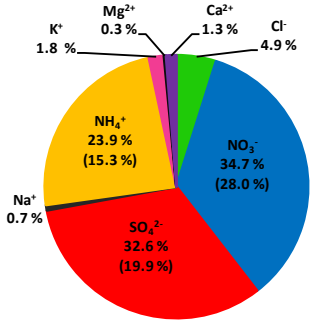

(b) Haze events: $PM_{2.5}$ = 171 ± 18 μg m^{-3}

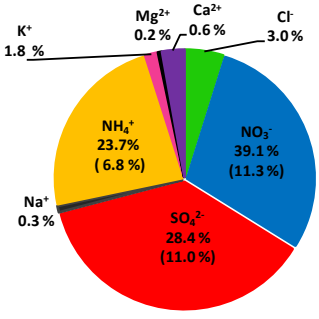

(c) Clear events: $PM_{2.5}$ = 22 ± 9 μg m^{-3}

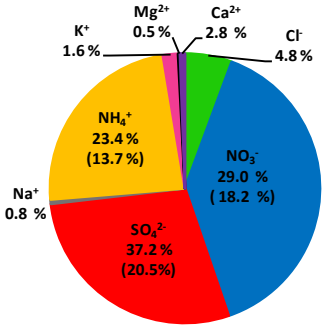

Figurer 3 Abundance of each species in TWSIIs during the (a) entire, (b) haze ($PM_{2.5}$ ≥ 150 μg m^{-3}) and (c) clear ($PM_{2.5}$ < 35 μg m^{-3}) events. The numbers in the parentheses are standard deviations.

https://doi.org/10.5194/acp-2019-752
Preprint. Discussion started: 4 September 2019

Atmospheric Chemistry and Physics Discussions

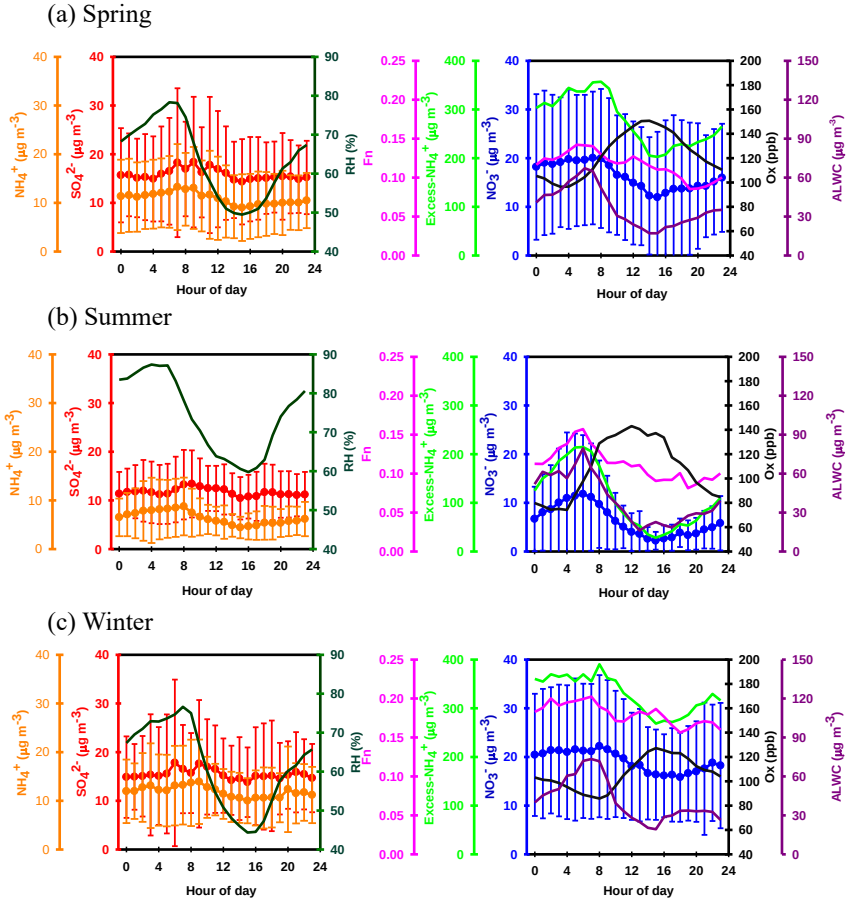

Figure 4 Diurnal variations of the concentrations of NO_3^-, SO_4^{2-} and NH_4^+, excess-NH_4^+, Ox and ALWC, and nitrogen conversion ratio (Fn) as well as ambient relative humidity in Nanjing during the sampling periods. For SO_4^{2-}, NO_3^- and NH_4^+, the mean values (dots) and standard deviations (solid lines) are plotted.

https://doi.org/10.5194/acp-2019-752
Preprint. Discussion started: 4 September 2019

Atmospheric Chemistry and Physics Discussions

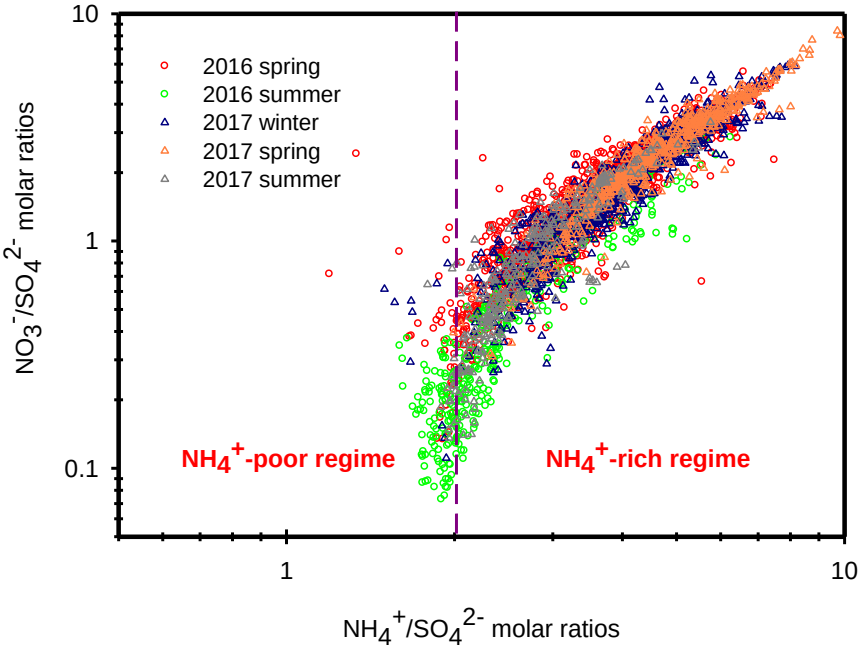

Figure 5 Scatter plots of molar ratios of NO_3^-/SO_4^{2-} against NH_4^+/SO_4^{2-} in Nanjing during the different seasons.

https://doi.org/10.5194/acp-2019-752
Preprint. Discussion started: 4 September 2019

Atmospheric Chemistry and Physics Discussions

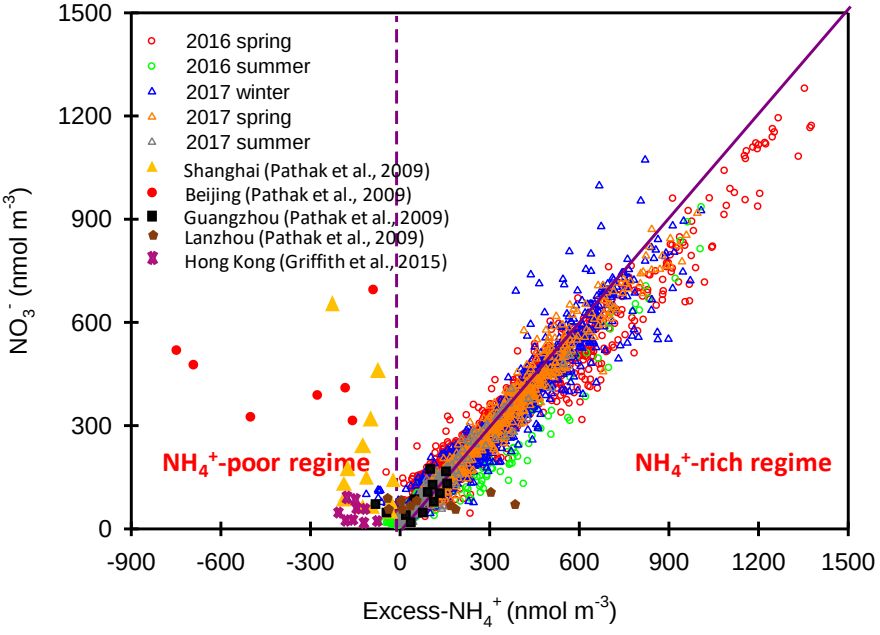

Figure 6 Scatter plot of NO_3^- vs. excess-NH_4^+ molar concentrations in Nanjing during the different seasons. The results in Beijing, Shanghai, Guangzhou, Lanzhou and Hong Kong are also shown in this figure.

https://doi.org/10.5194/acp-2019-752
Preprint. Discussion started: 4 September 2019

Atmospheric Chemistry and Physics Discussions

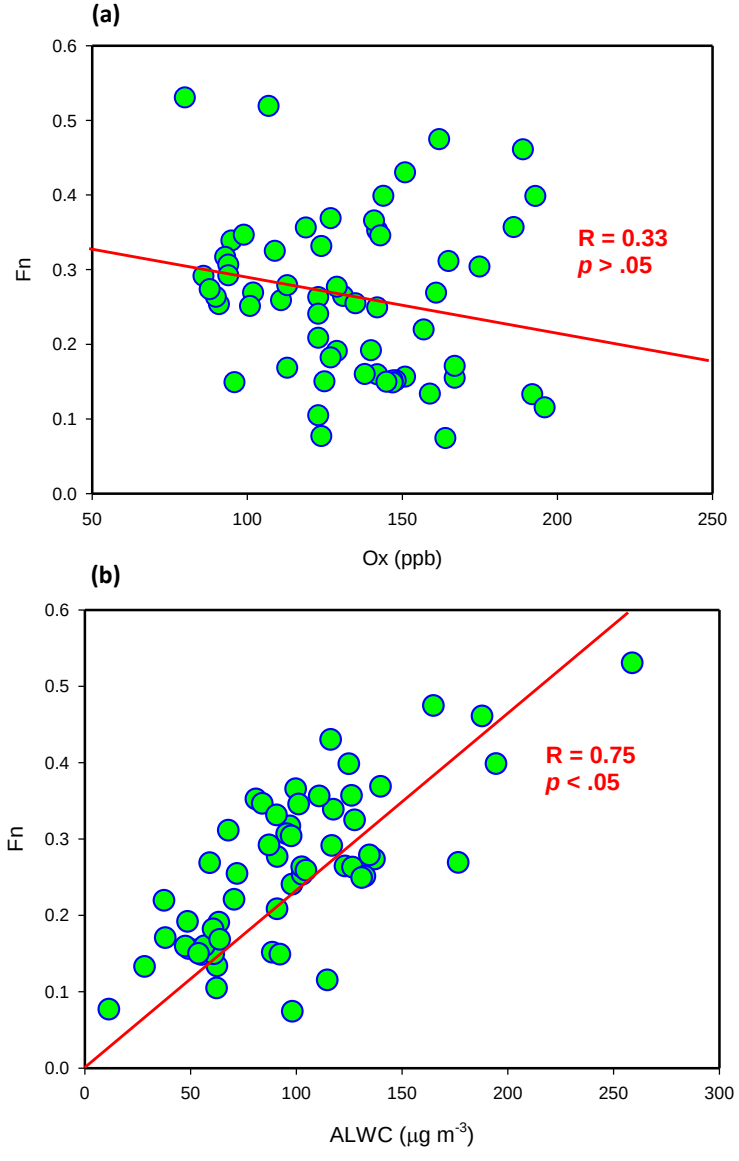

Figure 7 Scatter plots of (a) Fn against Ox and (b) Fn against ALWC during the high hourly $PM_{2.5}$ concentration conditions (hourly $PM_{2.5}$ ≧ 150 μg m^{-3}).

https://doi.org/10.5194/acp-2019-752
Preprint. Discussion started: 4 September 2019

Atmospheric Chemistry and Physics Discussions

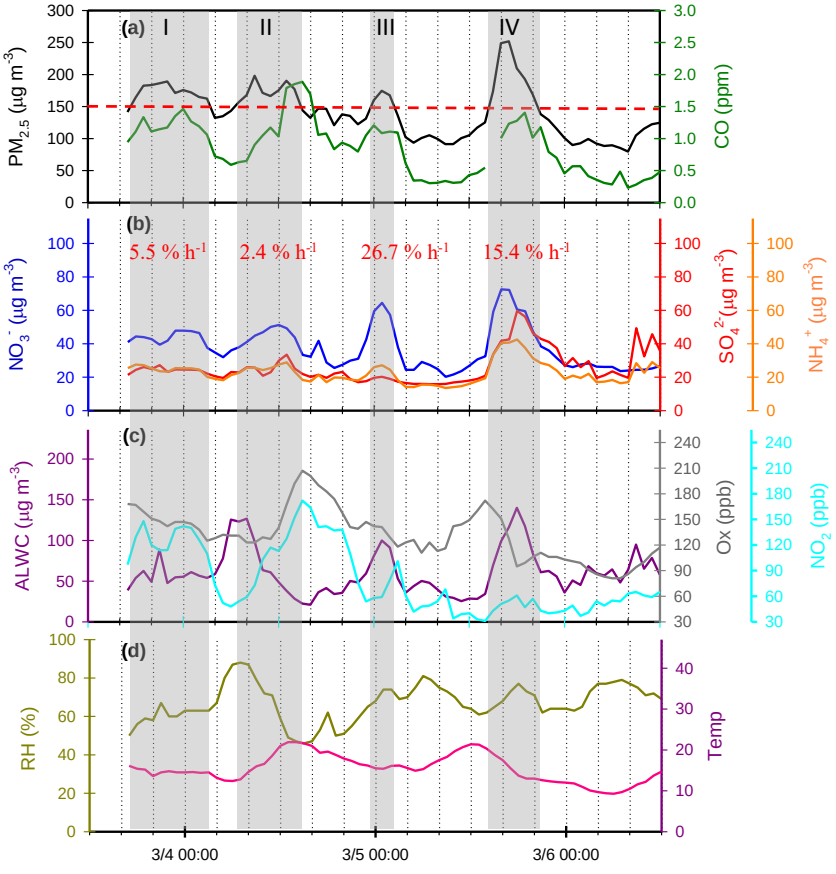

Figure 8 Time series of concentrations in (a) $PM_{2.5}$ mass and CO, (b) SIA species (NO_3^-, SO_4^{2-} and NH_4^+), (c) ALWC, Ox and NO_2 and (d) RH and T in Nanjing City from March 3 to 6, 2016. The grey shadows denote $PM_{2.5}$ episodes. The red numbers represent NO_3^- formation rate during the $PM_{2.5}$ episodes.

https://doi.org/10.5194/acp-2019-752
Preprint. Discussion started: 4 September 2019

Atmospheric Chemistry and Physics Discussions

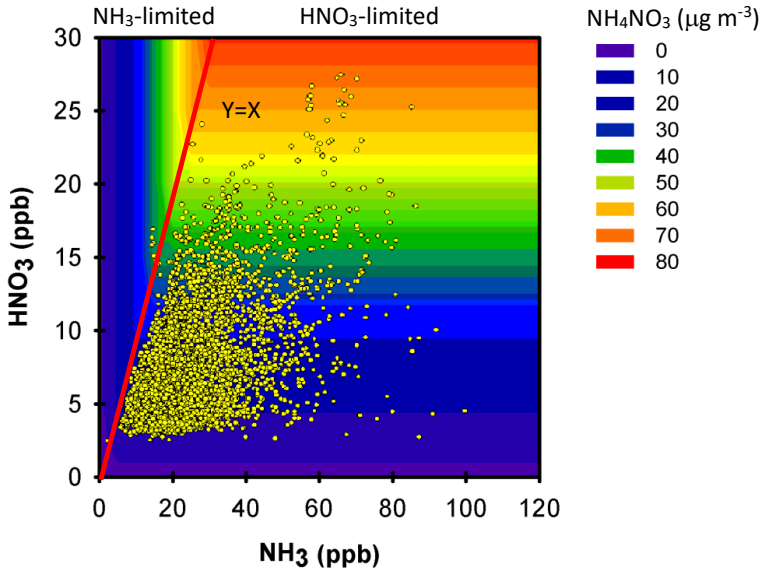

Figure 9 The isopleth of concentration in NH_4NO_3 aerosols ($\mu g\ m^{-3}$) versus NH_3 and HNO_3 concentrations (units in ppb). The NH_4NO_3 concentrations were calculated using Eq. 2 in the text. The dots denote the observed data.